Physics Letters A 377 (2013) 582–586

Contents lists available at SciVerse ScienceDirect

Physics Letters A

www.elsevier.com/locate/pla

Optical gain spectra of unstrained graded GaAs/$Al_xGa_{1-x}As$ quantum well laser

E.L. Albuquerque [a], U.L. Fulco [a,*], M.S. Vasconcelos [b], P.W. Mauriz [c]

[a] Departamento de Biofísica e Farmacologia, Universidade Federal do Rio Grande do Norte, 59072-970 Natal, RN, Brazil
[b] Escola de Ciências e Tecnologia, Universidade Federal do Rio Grande do Norte, 59072-970 Natal, RN, Brazil
[c] Departamento de Física, Instituto Federal de Educação, Ciência e Tecnologia do Maranhão, 65020-300 São Luís, MA, Brazil

ARTICLE INFO

Article history:
Received 10 August 2012
Received in revised form 11 December 2012
Accepted 13 December 2012
Available online 28 December 2012
Communicated by R. Wu

Keywords:
Lasers
Quantum wells
Optical gain
Luttinger–Kohn method
Abrupt/non-abrupt interfaces

ABSTRACT

We have calculated the optical gain spectra in unstrained graded GaAs/$Al_xGa_{1-x}As$ single quantum well lasers as a function of the energy of the radiation, the quantum well width and the interface thickness. The optical gain spectra were calculated using the density matrix approach (Luttinger–Kohn method), considering the parabolic band model (conduction band), all subband mixing between the heavy and light holes (valence band), and the transversal electrical light polarization. Our results show that the optical peak gain is sensitive to the width and the graded profile of the interfaces, and is blue-shifted as a function of the interface width.

It is widely acknowledge that the importance of lasers is typically reflected due to their practical use in a large range of applications, as well as their highly controllable nonlinear coherent optical response [1,2]. To accomplish this task, there is a systematic effort nowadays, to reduce the required injection for the onset of lasing. This is done mainly by means of a dynamic exchange of energy between the carriers (electrons and holes) and photons in a resonant cavity, leading to relaxation oscillations, whenever the carrier population is perturbed by an external source such as an electrical injection or optical excitation [3,4].

In a semiconductor laser, relaxation oscillations give rise to deleterious effects, such as linewidth enhancement and chirp, due to the periodic modification of the refractive index in the active gain region by the carrier concentration modulation. Fortunately, these effects can be minimized by fabricating structures of reduced dimensionality, such as quantum wells, wires, and dots [5,6]. Other possibility is to take into account physical mechanisms that enhance stimulated emission, such as polaritons, allowing the development of a new generation of ultralow power and ultracompact room-temperature photonic devices [7–10]. The introduction of spin-polarized carriers may also present a valuable model system to elucidate the recombination of the carrier population, which plays an important role in the operation of a conventional laser [11]. Radiative recombination of spin-up and spin-down carriers in the active region of any semiconductor light source produces left- and right-circularly polarized light, respectively, giving rise to two equal and in-phase circularly polarized modes. Injection of spin-polarized carriers leads to emission of circularly or elliptically polarized light via the selection rules for radiative recombination [12,13].

Semiconductor lasers have been attractive for research because they are both physically very interesting and technologically important [14–16]. This is especially true for quantum well lasers, where it is possible to control the range, depth, and arrangement of the quantum mechanical potential wells, opening up the possibility to make very good devices [17–19]. The importance of the quantum well laser has steadily grown until today, where it is preferred for most semiconductor laser applications. This growing popularity is because, in almost every aspect, the quantum well laser is somewhat better than the conventional one with bulk active layers [20–22].

With the ability to grow different semiconductor layers epitaxially with atomic precision in thickness, the material bandgap can be designed to confine electrons in much the same way as described in standard quantum mechanics textbooks. This quantum confinement of the electron along the growth direction, significantly alters the band structure of the semiconductor, changing almost every property of the material to one degree or other [23]. The optical gain becomes dependent on the confinement characteristics of the semiconductor systems, in which the interfaces play a significant role.

* Corresponding author. Tel.: +55 84 32153793; fax: +55 84 32153791.
E-mail address: umbertofulco@gmail.com (U.L. Fulco).

0375-9601/$ – see front matter
http://dx.doi.org/10.1016/j.physleta.2012.12.025

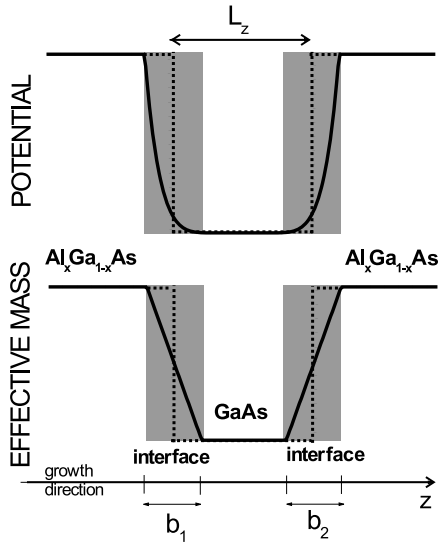

Fig. 1. Schematic illustration of the effective mass and potential energy of a GSQW (solid line) and of the equivalent abrupt ASQW (dotted line).

Investigations on the abrupt quantum well (QW) structures have been widely reported, although the use of less-abrupt interfaces in QW structures are relatively new. Recent works had shown the importance of using QWs with graded and less-abrupt interfaces in InGaN-based material systems, looking for improved spontaneous emission rate [24–26] and improved optical gain [27]. Besides, the improvement in quantum confined Stark effect had also been reported in Gaussian shape QWs [28], as well as the use of quantum well intermixing to form the less-abrupt interfaces leading to large blue-shift in emission wavelength [29].

The unstrained GaAs QWs structures are employed primarily as active regions for 850-nm diode lasers and vertical cavity surface emitting lasers, which are used as optical transmitters in datacom applications. However, several works considering compressively-strained InGaAsP QWs [30] and narrow InGaAs QWs [31] had been also used as improved active regions for achieving high performance 850-nm emitting lasers operating at high temperature with large differential gains attributed to their large compressive strain in the QWs. As a consequence, they depict very low-threshold current density [32] due to its large optical gain [33].

It is the aim of this work to describe a theoretical calculation of the optical gain in unstrained graded single quantum well (GSQW) lasers GaAs/$Al_xGa_{1-x}As$, as a function of the energy of the radiation, of the interface thickness, and of the width of the quantum well. We consider only the transversal electrical (TE) light polarization since, although straightforward, no new results are found for the simplest transversal magnetic (TM) light polarization. The theoretical calculation was done considering all subbands transitions in the quantum well. The results are compared with the equivalent abrupt single quantum well (ASQW) laser (see Fig. 1 for details of the geometries).

To calculate the energy levels of the electrons and holes confined into a GSQW/ASQW, we use the multi-band effective mass theory and the envelope-function approach together with a transfer-matrix technique. For simplicity, the conduction and valence bands are considered decoupled, as usual for most III–V semiconductors. We consider also the envelope functions to be slowly varying over the unit cells of the lattice, and the z-axis as the material growth direction. The effective mass and gap energy have a dependence on z in the quantum well interfaces whose profile, as depicted schematically in Fig. 1 for a GSQW (solid line), is [34]:

$$m_i(z) = m_0\big[\mu_{1i} + \mu_{2i}|z|\big], \tag{1}$$

$$V_i(z) = Q_i\big[1 + \varepsilon_1|z| + \varepsilon_2 z^2\big], \tag{2}$$

where m_0 is the free-electron mass, with $i = e$ (electrons), lh (light holes) and hh (heavy holes). Also, $\mu_{1e} = 0.067$, $\mu_{2e} = 0.083$; $\mu_{1lh} = 0.087$, $\mu_{2lh} = 0.063$; $\mu_{1hh} = 0.62$, $\mu_{2hh} = 0.14$, $\varepsilon_1 = 1.155$, and $\varepsilon_2 = 0.37$ are experimental parameters related with the dependence on the aluminium molar fraction x of the $Al_xGa_{1-x}As$ effective mass and energy gap, respectively, at the Γ-symmetry point [34]. Q_i is the band offset for the ith type of carrier, whose values taken from experiments are $Q_e = 0.6$, $Q_{hh} = Q_{lh} = 0.4$. Fig. 1 also shows the profile (dotted line) of the equivalent abrupt single quantum well (ASQW) used in this work.

Within the effective mass approximation and with the assumption that the conduction band is parabolic, the electron envelope function can be considered independent of $\vec{k}_t = (k_x, k_y, 0)$, the in-plane wave vector, which is perpendicular to the z-axis. The energy of an electron on the nth conduction subband can be written as:

$$E_{en}(k_t) = E_c + E_{en}(0) + \frac{\hbar^2 k_t^2}{2m_{av,e}}, \tag{3}$$

where E_c is the conduction band-edge energy, k_t is the magnitude of $\vec{k}_t = (k_x, k_y, 0)$ and $m_{av,e}$ is a weighted average of the bulk electron effective mass, defined as:

$$[m_{av,e}]^{-1} = \frac{\int_{-\infty}^{\infty} |F_{en}(z)|^2 [m_e(z)]^{-1}\, dz}{\int_{-\infty}^{\infty} |F_{en}(z)|^2\, dz}. \tag{4}$$

Here, $F_{en}(z)$ is the zone-center ($k_t = 0$) envelope function that describes the motion of the electron on the growth direction of the nth conduction subband. Also, $E_{en}(0)$ is the subband-edge energy ($k_t = 0$), which satisfies the one-dimensional Schrödinger-like equation

$$H_e(z) F_{en}(z) = E_{en}(0) F_{en}(z), \tag{5}$$

whose confinement Hamiltonian is given by

$$H_e(z) = -\frac{\hbar^2}{2}\frac{d}{dz}\left[\frac{1}{m_e(z)}\frac{d}{dz}\right] + V_e(z). \tag{6}$$

In the above equation, $m_e(z)$ and $V_e(z)$ are the effective mass and the confinement potential of the electron, respectively, which are dependent on the coordinate z at the interface, according to Eqs. (1) and (2). Eq. (5) can be solved numerically using a transfer-matrix technique [35].

For the calculation of the energy levels and envelope functions of the holes, we shall take into account the mixing of the subbands of the light hole and heavy hole in the valence band structure. This effect is well described by a multi-band effective mass approximation based on the $\vec{k}\cdot\vec{p}$ method of Luttinger and Kohn [36]. We adopt an analog effective Hamiltonian approach described in [37] to calculate the valence subband structure. In this approach, the hole envelope functions $F_{hn}(k_t, z)$, corresponding to the energy $E_{hn}(k_t)$ at any finite k_t, is expressed as a linear combination of the envelope functions at $k_t = 0$ in the following way:

$$F_{hn}(k_t, z) = \sum_{n'=1}^{4M} A_{n'n}(k_t) F_{hn'}(0, z). \tag{7}$$

Here, $h = hh, lh$, with the first index denoting a doubly degenerate group of heavy-hole subbands, and the second one denoting a doubly degenerate group of light-hole subbands. Also, M is the number of levels of the heavy/light holes, and $F_{hn}(0, z)$ is the zone-center ($k_t = 0$) envelope function, which describe the motion of the respective h-hole on the growth direction of the nth